Supporting Information

Su et al. 10.1073/pnas.0902386106

Experimental

Circular Dichroism (CD) Experiments. Formation of G-quadruplexes was monitored by CD. Samples were measured immediately after the preparation or after storage for hours to days at 4 °C. All of the CD spectra were recorded on a J-810 spectropolarimeter (Jasco). The measurements were carried out with 100 μL 50 μM ODN samples in a 1-mm path quartz cell at 4 °C under nitrogen to prevent water condensation. Spectra shown (Fig. S1) were the average of 3 accumulations in a range from 220 to 300 nm with a band width of 1 nm, response time of 1 s, data pitch of 0.2 nm, and scan speed of 50 nm/min. A blank sample of 10 mM Tris·HCl buffer, pH 7.5, with 150 mM KCl or NaCl was used for baseline correction. The CD spectra for Tel22 in Na^+ (Fig. S1*A*) most closely matched those reported by Li et al., Xu et al., and Gray et al. (1–3) but differed from those reported by Ambrus et al. and Vorlickova et al. (4, 5) in the relative magnitude of the 263 nm peak to the 297 nm peak. Likewise, the spectra for Tel22 in K^+ (Fig. S1*B*) most closely matched those reported by Ambrus et al., Vorlickova et al., and Gray et al. (3–5) but differed somewhat from that reported by Li et al. (1) and more so from that reported by Xu et al. (2). These differences, their origin, or their significance, have not, to our knowledge, been addressed in the literature. The CD spectrum for Tel26 in K^+ (Fig. S1*C*) matched closely to that reported by Ambrus et al. (4).

Polyacrylamide Gel Electrophoresis (PAGE) Experiments. The 5′ termini of the oligodeoxynucleotides were labeled by a forward reaction with 1× reaction buffer (500 mM Tris·HCl, pH 7.6, 100 mM $MgCl_2$, 50 mM DTT, 1 mM spermidine, 1 mM EDTA; Fermentas Life Science) with 10 U T4 polynucleotide kinase and 20 pmol [γ-^{32}P]-ATP at 37 °C for 30 min. The reaction was quenched by adding to an equal volume of 2× loading buffer (98% formamide, 10 mM EDTA), boiling for 2 min, and cooling on ice for another 1 min. The radiolabeled samples were then analyzed on a 15% denaturing polyacrylamide gel and scanned with a PhosphorImager (Bio-Rad Laboratories).

1. Li J, Correia JJ, Wang L, Trent JO, Chaires JB (2005) Not so crystal clear: The structure of the human telomere G-quadruplex in solution differs from that present in a crystal. *Nucleic Acids Res* 33:4649–4659.
2. Xu Y, Noguchi Y, Sugiyama H (2006) The new models of the human telomere d[AGGG(TTAGGG)3] in K+ solution. *Bioorg Med Chem* 14:5584–5591.
3. Gray RD, Li J, Chaires JB (2009) Energetics and kinetics of a conformational switch in G-quadruplex DNA. *J Phys Chem B* Jan 5. [Epub ahead of print].
4. Ambrus A, et al. (2006) Human telomeric sequence forms a hybrid-type intramolecular G-quadruplex structure with mixed parallel/antiparallel strands in potassium solution. *Nucleic Acids Res* 34:2723–2735.
5. Vorlickova M, Chladkova J, Kejnovska I, Fialova M, Kypr J (2005) Guanine tetraplex topology of human telomere DNA is governed by the number of (TTAGGG) repeats. *Nucleic Acids Res* 33:5851–5860.

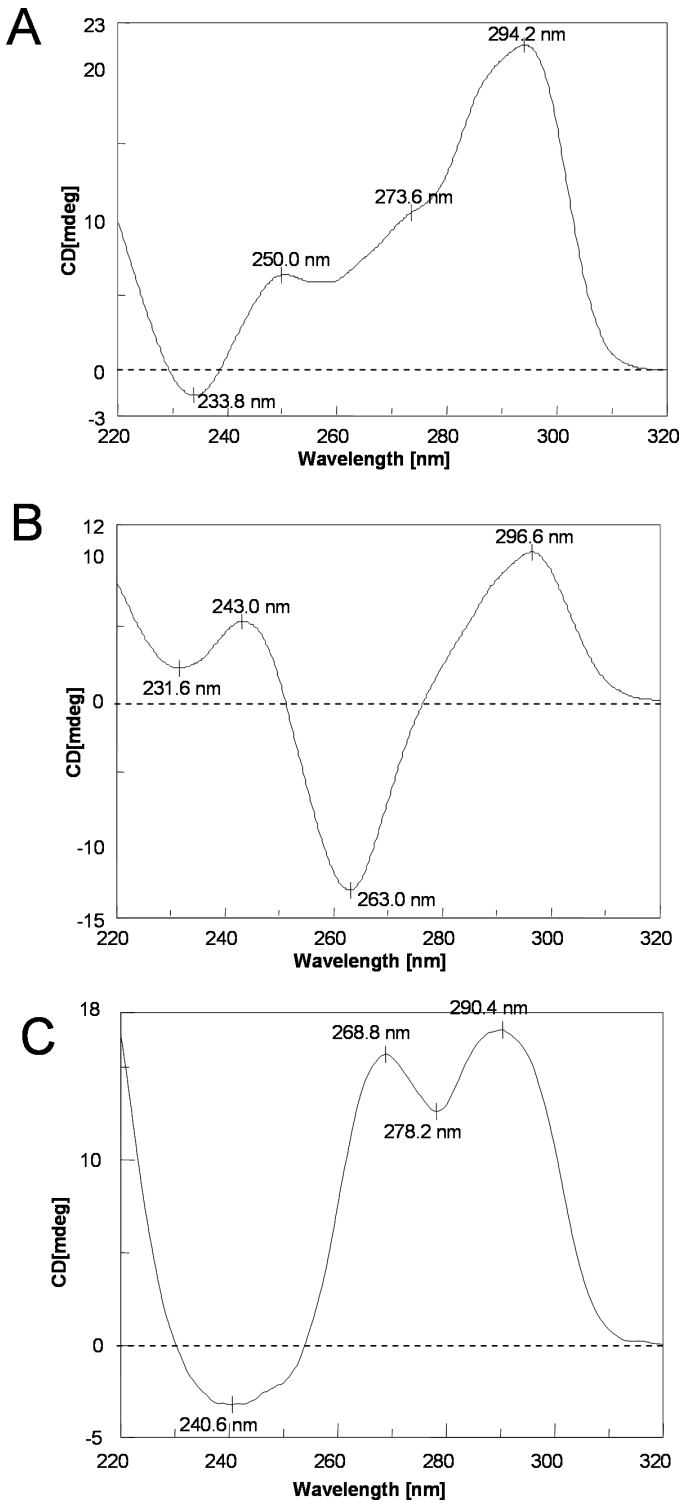

Fig. S1. CD spectra of 50 μM Tel22 G-quadruplexes in 10 mM Tris·HCl, pH 7.5, at 4 °C. (*A*) Tel22 in 150 mM K^+ solution after denaturing and renaturing process. (*B*) Tel22 in 150 mM Na^+ solution after denaturing and renaturing process. (*C*) CD spectrum of 50 μM Tel26G-quadruplex at 4 °C after 24 h.

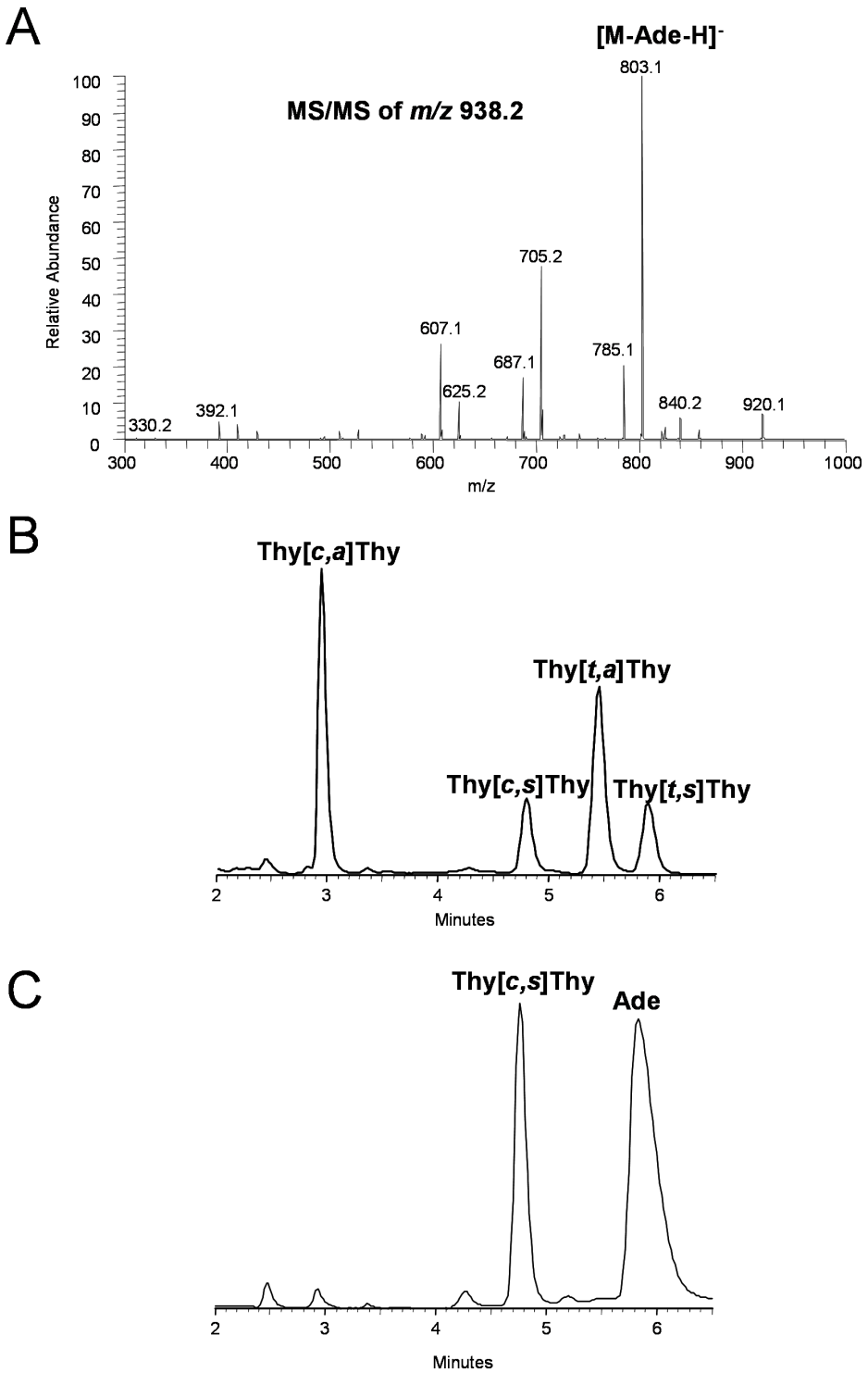

Fig. S2. ESI-MS/MS and HF/pyridine hydrolysis assay of HPLC peak 3. (*A*) ESI-MS/MS of peak 3, (*B*) HPLC of authentic thymine cyclobutane dimers, and (*C*) HF/pyridine hydrolysis-coupled HPLC assay of peak 3.

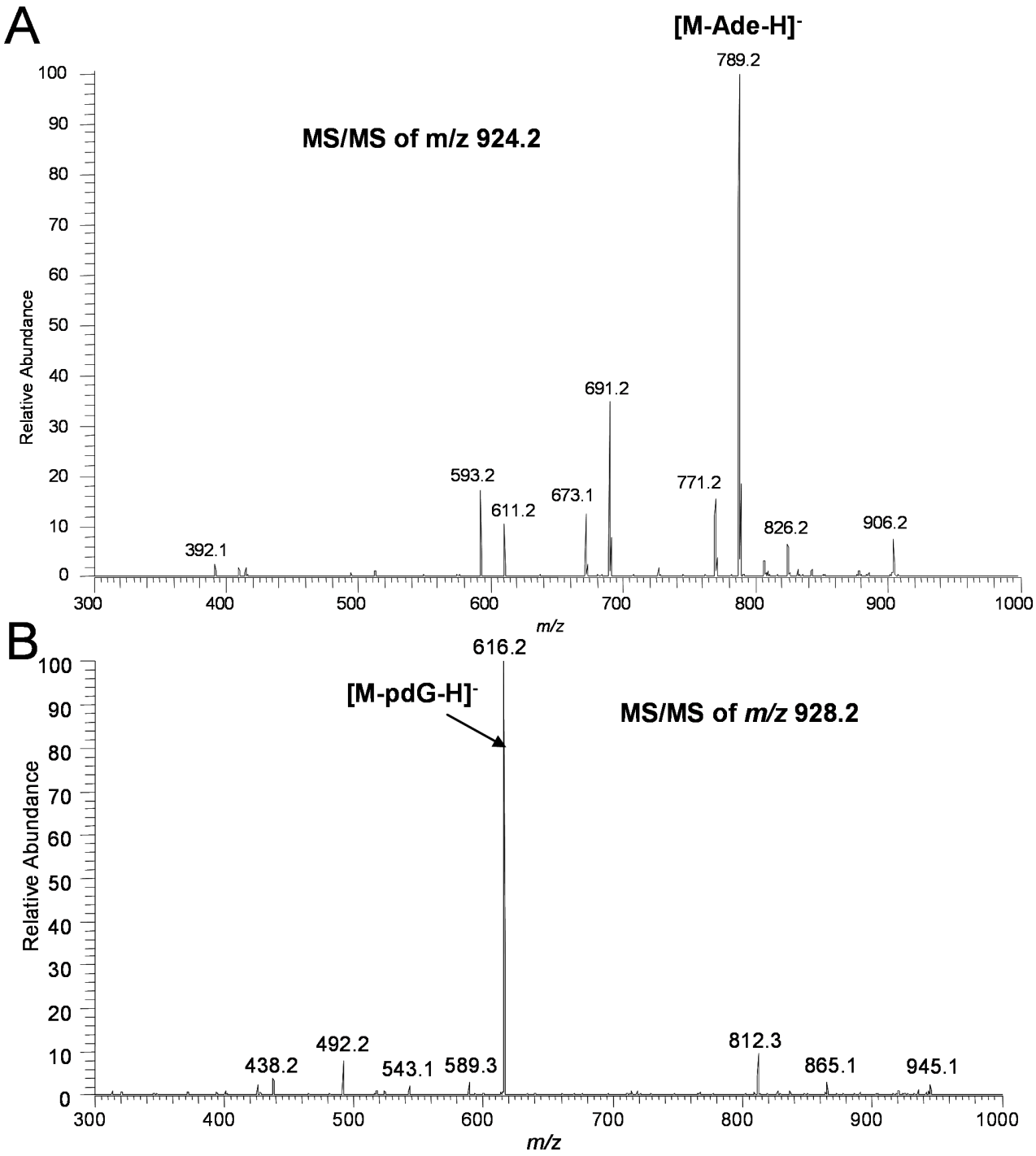

Fig. S3. ESI-MS/MS of (*A*) HPLC peak *n*-1 (*n* = 1, 2, and 3), pd[T = UA] and (*B*) HPLC peak *n*-2 (*n* = 1, 2, and 3), pd[T = AG] corresponding to the TA* photoproduct.

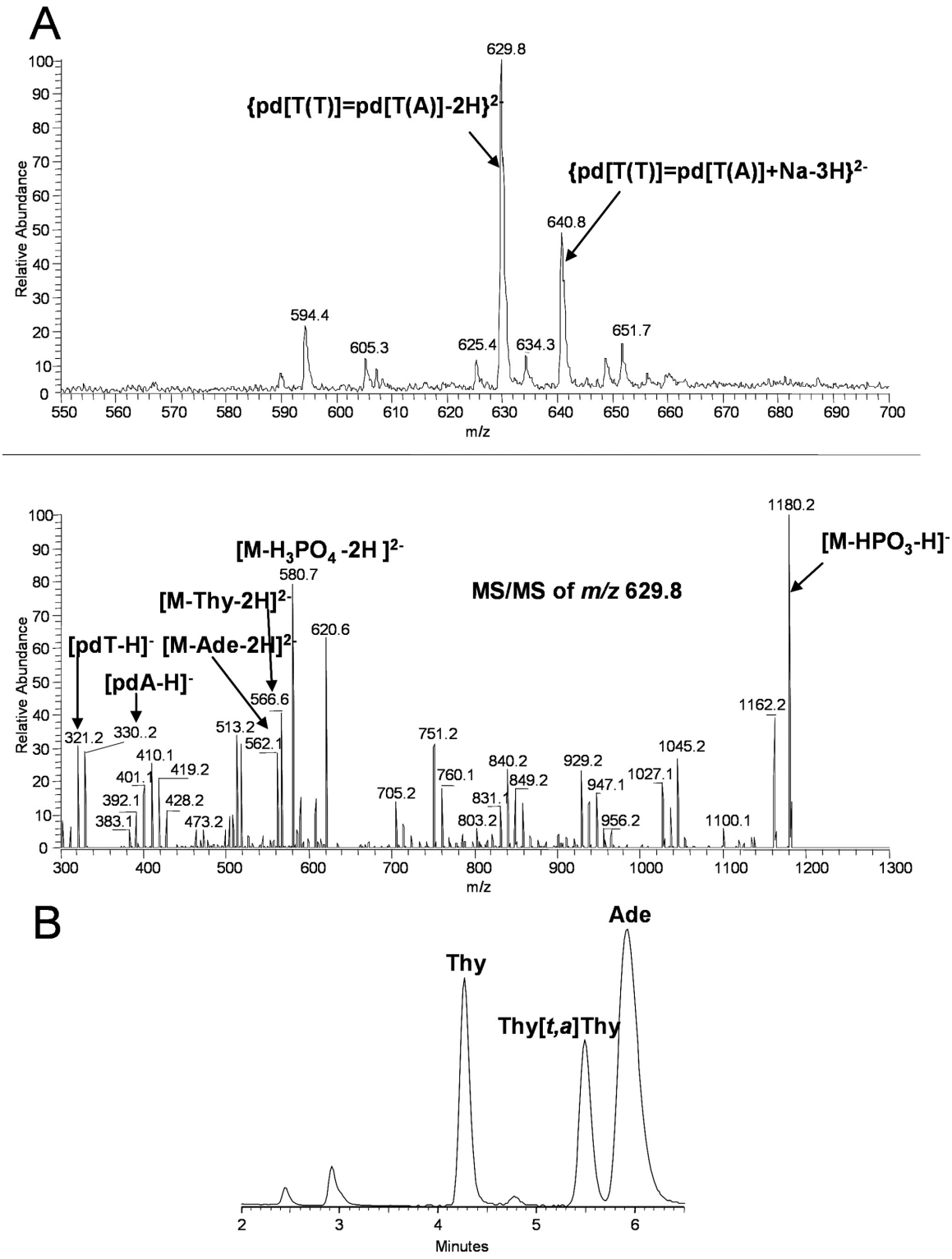

Fig. S4. ESI-MS, ESI-MS/MS, and HF/pyridine hydrolysis-coupled HPLC assay of HPLC peak 11. (*A*) ESI-MS and MS/MS. (*B*) HF/pyridine hydrolysis-coupled HPLC.

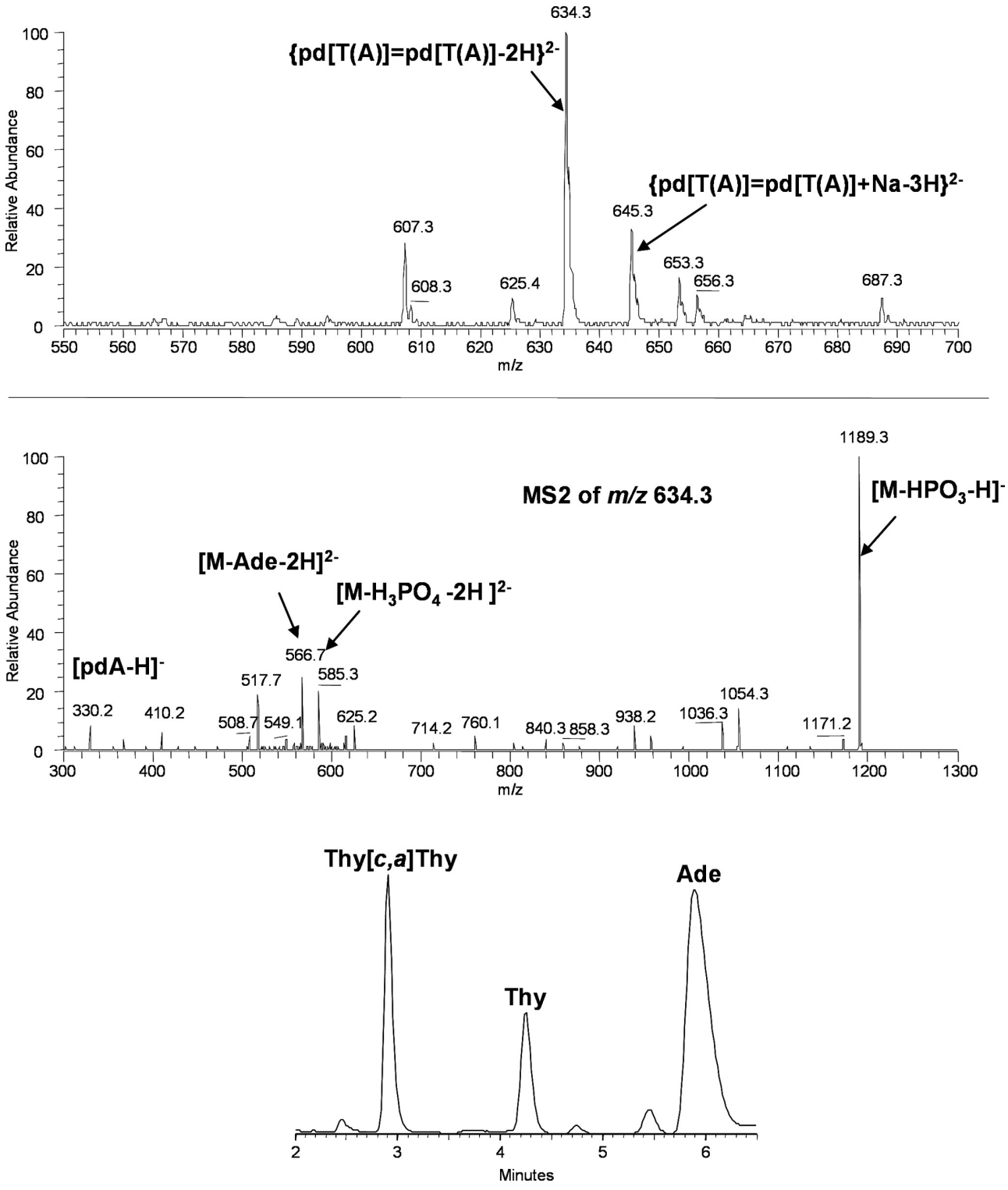

Fig. S5. ESI-MS, ESI-MS/MS, and HF/pyridine hydrolysis-coupled HPLC assay of HPLC peak 9. (*A*) ESI-MS and MS/MS. (*B*) HF/pyridine hydrolysis-coupled HPLC assay.

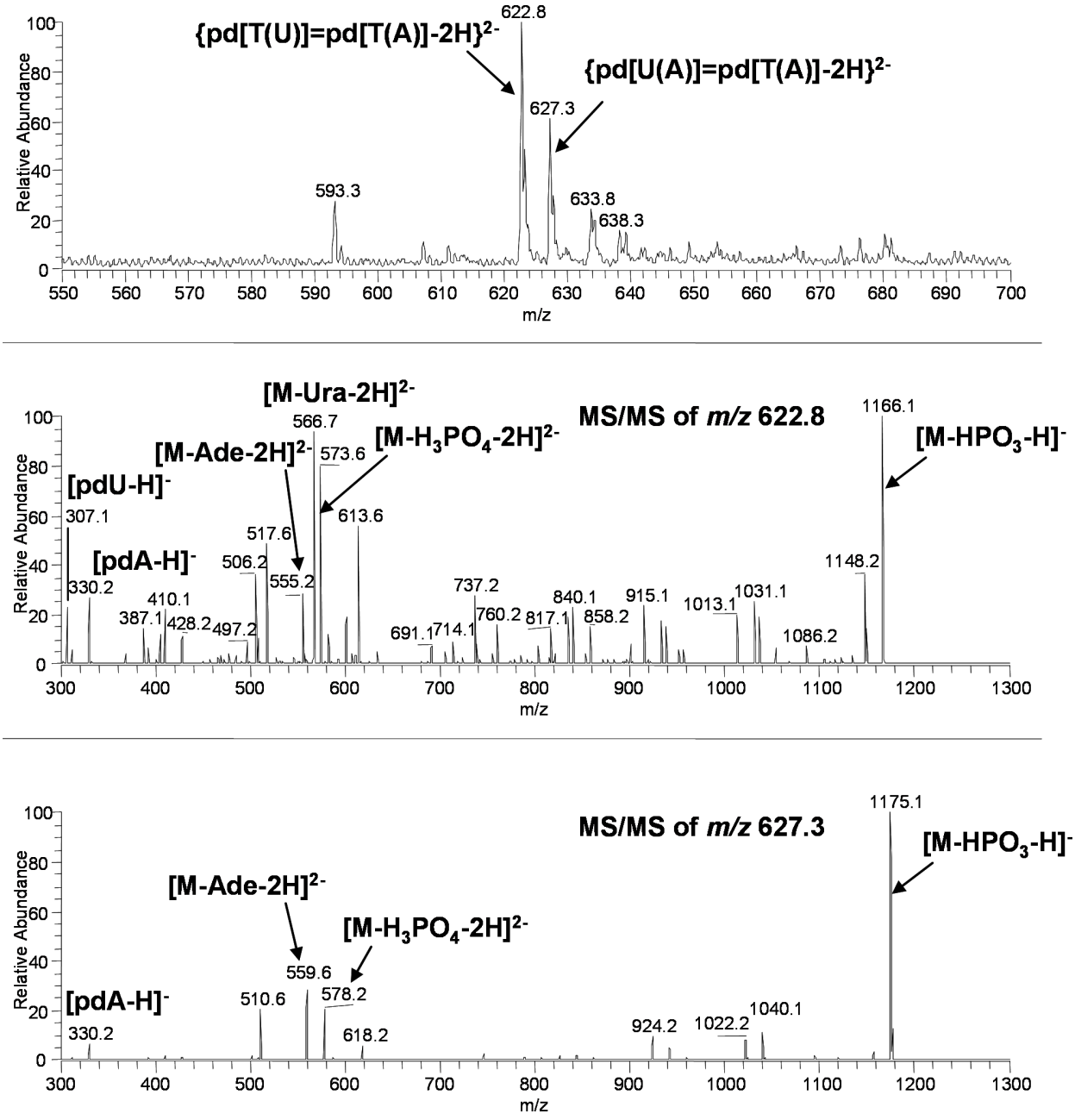

Fig. S6. ESI-MS and ESI-MS/MS of HPLC peak 1-6.

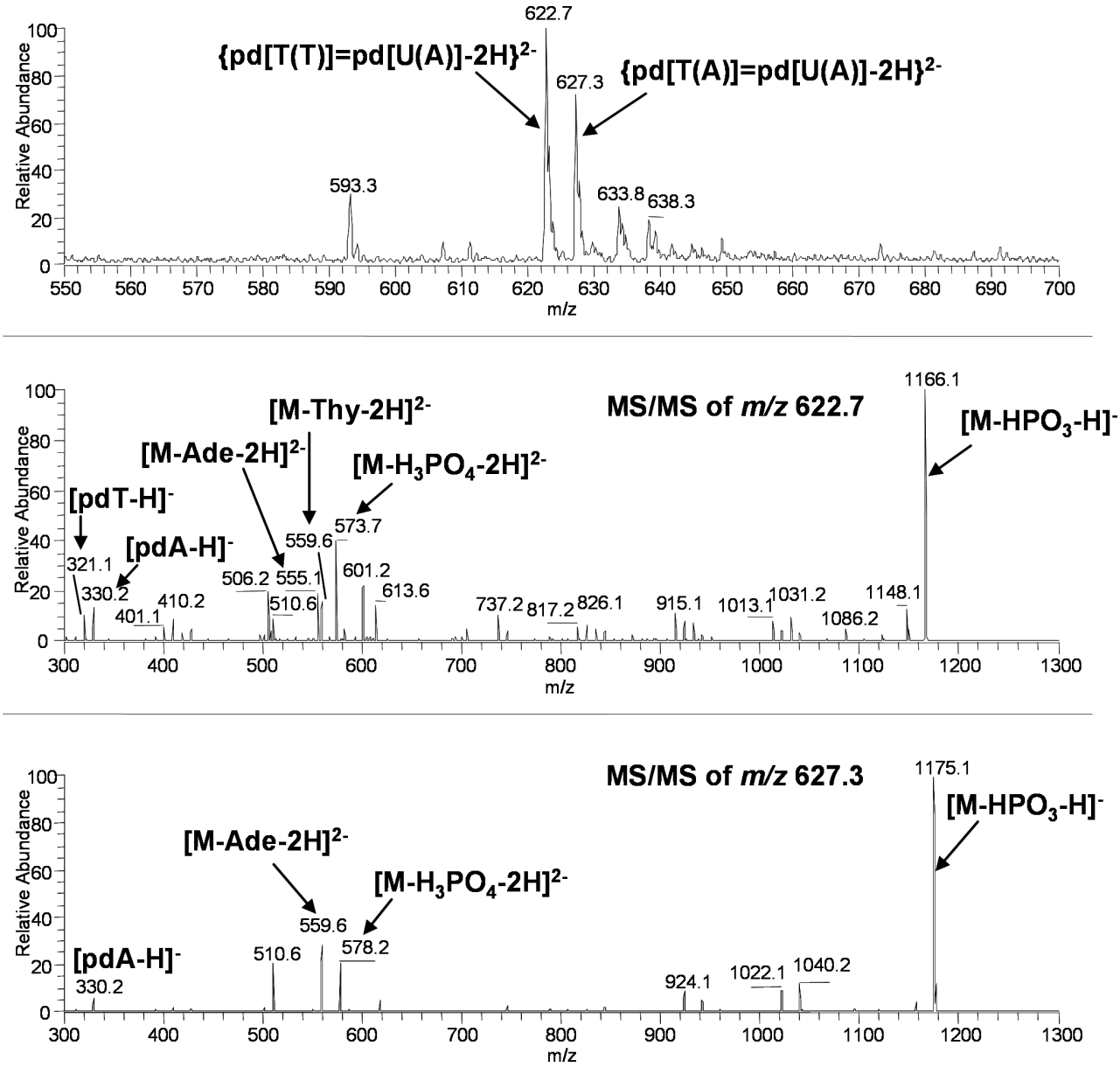

Fig. S7. ESI-MS and ESI-MS/MS of HPLC peak 3-6.

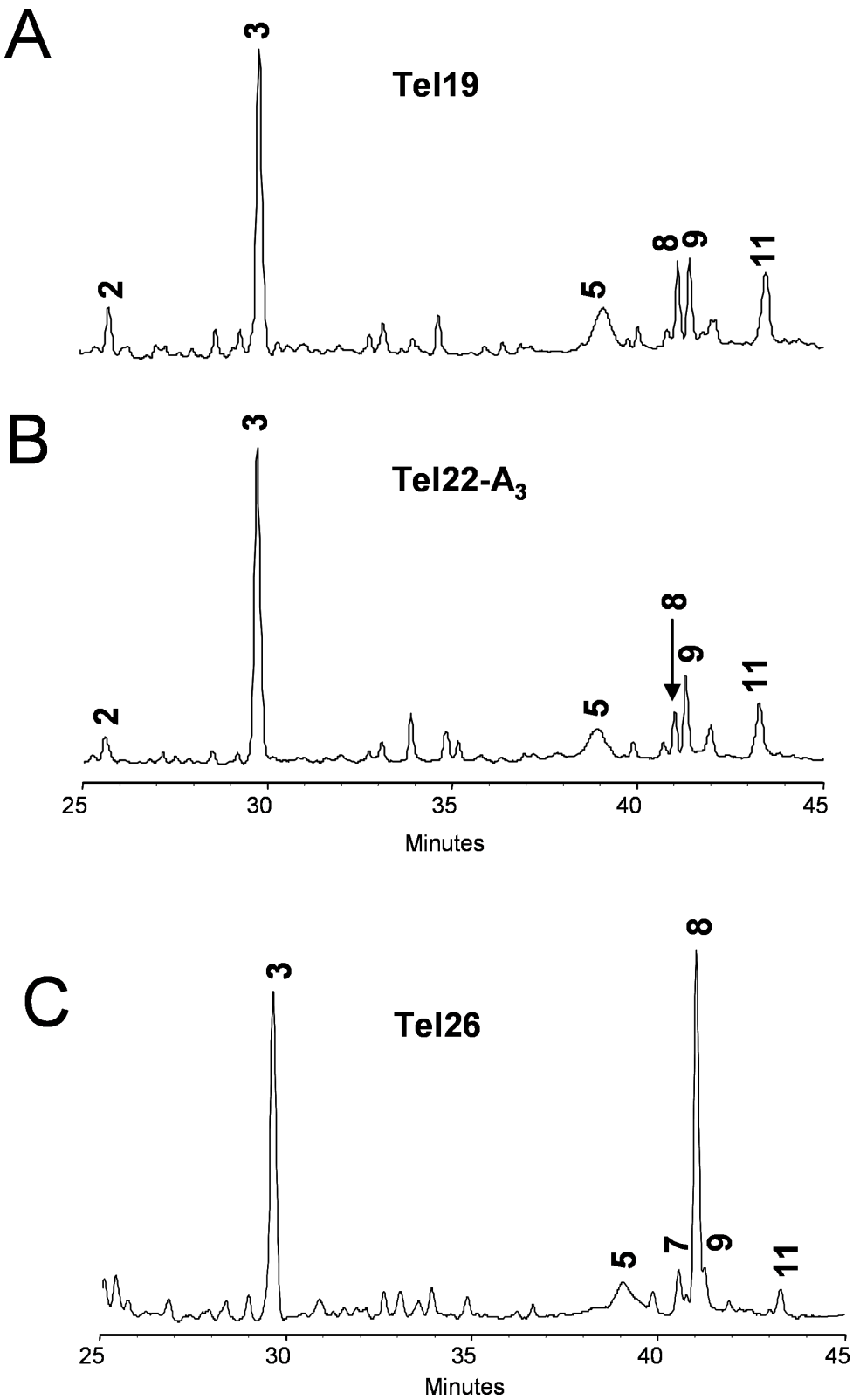

Fig. S8. NP1-coupled HPLC assay of UV-irradiated Tel19, Tel 22-A_3, and Tel26. (*A*) Tel19 in K^+ solution after 2.5 h UVB irradiation. (*B*) Tel 22-A_3 in K^+ solution after 2.5 h UVB irradiation. (*C*) NP1-coupled HPLC assay of Tel26in K^+ solution (see Fig. S1*C*) after 2.5 h UVB irradiation. *anti* dimers of Tel26 were mapped to loops 1 and 3 by replacement with U.

Table S1. Stereochemistry, composition, and loop assignment of the NP1 digestion products of Tel22-U^n (n = 1, 2, 3) in Fig. 4*C*, *D*, and *E*

HPLC peak	Stereochemistry	Base composition
1-1, 2-1, 3-1	—	T=UA
1-2, 2-2, 3-2*	—	T=AG
1-3, 2-3, 3-3*	*c,s*	T=TA
1-4	—	U^1(A)=T(A)
		U^1(A)=T(T)†
1-5	—	T^1(U)=T(A)
		U^1(A)=T(A)
1-6	—	T^1(U)=T(A)
		U^1(A)=T(A)
1-8	—	U^1(A)=T(A)
		T^1(U)=T(A)†
1-12	—	U^1(A)=T(A)
2-5	—	T(A)=T^2(U)
		T(A)=U^2(A)
		T^1(T)=T^3(A)
		T^1(A)=T^3(A)
2-7*	*c,a*	T^1(A)=T^3(A)
2-8*	*t,a*	T^1(A)=T^3(A)
2-9*	*c,a*	T^1(A)=T^3(A)
2-10*	*c,a*;*t,a*‡	T^1(T)=T^3(A)
		T^1(A)=T^3(A)
2-11*	*t,a*	T^1(T)=T^3(A)
3-4	—	T(T)=U^3(A)
		T(A)=U^3(A)
3-5	—	T(A)=U^3(A)
		T(A)=T^3(U)§
3-6	—	T(T)=U^3(A)
		T(A)=U^3(A)
3-8	—	T(A)=T^2(A)
		T(A)=U^3(A)¶
		T(A)=T^3(U)¶
3-12	—	T(A)=U^3(A)

Loop assignment indicated by the superscripted number.
*Same products as assigned for Tel22 in Table 1.
†Less than 20% estimated from MS peak intensity.
‡Could not be assigned to a specific product.
§Less than 10% estimated from MS peak intensity.
¶Less than 15% estimated from MS peak intensity.